AIP Advances

New rule and growth model for the synthesis method of gold nanorods with binary surfactant CTAB and NaOL

Cite as: AIP Advances **12**, 085019 (2022); https://doi.org/10.1063/5.0100475
Submitted: 24 May 2022 • Accepted: 01 August 2022 • Published Online: 19 August 2022

Ming-Zhang Wei, Tian-Song Deng, Qi Zhang, et al.

View Online

Export Citation

CrossMark

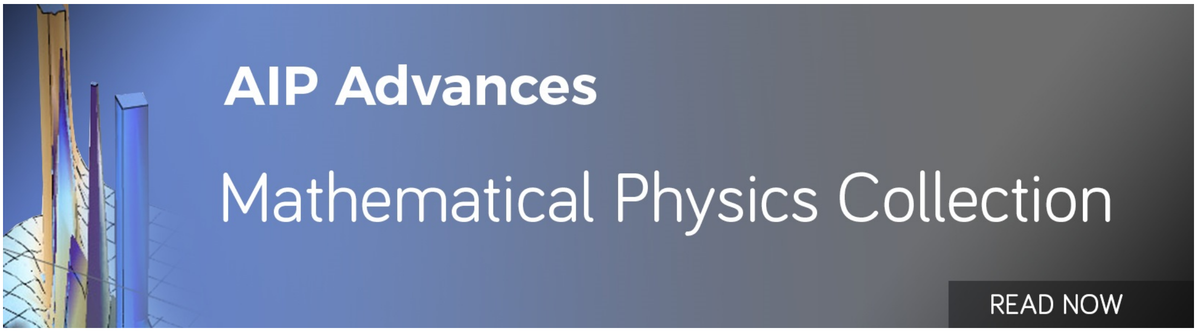

AIP Advances ARTICLE scitation.org/journal/adv

New rule and growth model for the synthesis method of gold nanorods with binary surfactant CTAB and NaOL

Cite as: AIP Advances 12, 085019 (2022); doi: 10.1063/5.0100475
Submitted: 24 May 2022 • Accepted: 1 August 2022 •
Published Online: 19 August 2022

Ming-Zhang Wei, Tian-Song Deng,[a)] Qi Zhang, Xi Chen, Zhiqun Cheng, Shiqi Li, and Yi-Jie Gu

AFFILIATIONS

College of Electronics and Information Engineering, Hangzhou Dianzi University, No. 1158, 2nd Avenue, Baiyang Street, Hangzhou 310018, China

[a)]**Author to whom correspondence should be addressed:** dengts@pku.edu.cn

ABSTRACT

The roles of CTAB and Ag^+ have been discovered and given us a deeper understanding of the seed-mediated method in the gold nanorods synthesis. Former work used binary surfactants CTAB + NaOL (sodium oleate) to greatly improve the dimensional tunability and monodispersity of gold nanorods. However, they only used a few of the concentration combinations of the binary surfactants, and the influence of NaOL under this method has not been systematically studied. In this work, we carried out systematic experiments under the variation of NaOL and used transmission electron microscopy and UV–vis-near-infrared spectroscopy to monitor the growth process of the gold nanorods. The results showed that the NaOL contributed to the symmetry breaking process. We discovered the ideal ranges of NaOL concentration under different concentrations of CTAB (10–40 mM). Lower concentrations of NaOL produced many impurities, such as Au spheres, while higher concentrations of NaOL led to the decrease of monodispersity of the obtained gold nanorods. A growth model based on the balance of diffusion/reduction of the growth solution has been proposed in order to explain the formation of the gold nanorods.

INTRODUCTION

Noble metal nanocrystals have drawn great attention in the research of nanomaterials for their specific physical/chemical properties corresponding to sizes, shapes, and surface effects. Among these nanocrystals, gold nanorods (AuNRs) have been widely studied and put into applications as representative branches in surface-enhanced Raman scattering (SERS),[1–4] biomedicine,[5–8] and imaging.[9–11] The unique optical properties of AuNRs at the nanoscale are due to the localized surface plasmon resonance (LSPR) effect, which is directly related to its aspect ratio (length/diameter). The LSPR comes from the polarization of free electrons on AuNR's surface caused by electromagnetic waves and only occurs when the lengths and diameters of AuNRs are much smaller than the wavelength of the electromagnetic waves. Each AuNR with different aspect ratios has a corresponding LSPR peak, from 600 nm to the near-infrared (NIR) region. The strongly shape-dependent characteristics of AuNRs rely on advanced synthetic methods for a wide range of scientific research and applications.[12] A significant "milestone" in the development of such a method for AuNRs synthesis was the so called seed-mediated growth, which was carried out by Nikoobakht and El-Sayed[13] by introducing Ag^+, for an optimization of the method purposed by Jana *et al.*[14] The growth process of AuNRs is under the combined effects of several molecules and ions. By fast reduction of the chloroauric acid with sodium borohydride, ~2 nm gold nanoparticles were prepared as seeds, which provided a template for slow overgrowth and catalyzing the reaction. Through the mild reduction of ascorbic acid (AA), the AuNRs were obtained. The surfactant CTAB is introduced in this process as a stabilizer and enhanced the anisotropic growth.[15]

In the past 20 years, many studies were carried out, aiming at exploring the roles and functions of chemicals in the synthesis of AuNRs, including the role of seed,[16] Ag^+ as shape controlling and yielding agents,[14,17] CTAB, and iodide for its formation process.[18,19]

Two other outstanding improvements for seed-mediated methods were further proposed by Murray's group.[20,21] They introduced sodium oleate (NaOL) as binary surfactants together with CTAB and successfully obtained AuNRs with both high monodispersity and tunability. In this method, the high concentration of AA in the growth solution is unnecessary because the Au^{3+} is reduced to Au^+ by the C=C double bond of the NaOL molecules at first. Moreover, the HCl is introduced to adjust the pH in the final growth solution. Hence, the reducibility of AA is constrained and limited by both acidic solution and the relatively low concentration. The LSPR peaks of the obtained AuNRs can be tuned from about 600 to 1200 nm by changing the amounts of $AgNO_3$, seeds, and/or HCl. Although the concentration of CTAB was dropped to 37 mM, the monodispersity of the obtained samples was greatly improved. Later, Xu *et al.*[22] carried out a series of experiments to get a better understanding of the cooperative interactions among CTA^+, Br^-, and Ag^+ under this binary surfactant (CTAB + NaOL) method and demonstrated that the most critical factor in the seeded growth of AuNRs is the complex, $CTA\text{-}Br\text{-}Ag^+$. Besides NaOL, Liz-Marzán *et al.*[23] also used n-decanol as the secondary surfactant in the symmetry breaking process.

However, Murray's work provided only two fixed concentrations of NaOL (8 and 11 mM) as the standard and reference of this method. It is still unclear whether the combinations of the binary surfactant are the optimal situation. In our recent work, we found that the minimum value of the CTAB concentration can be as low as 10 mM while maintaining the tunability and monodispersity of the obtained AuNRs. We dropped the NaOL concentration to 5 mM because the samples synthesized at 8 and 11 mM of NaOL were failed under this low CTAB situation.[24] Are there any trends or rules for NaOL concentration under different synthesis situations? In this work, to expand this binary surfactant method, we carried out systematic experiments to discover the influence of NaOL in the seed-mediated synthesis of AuNRs, including the ideal NaOL concentrations under a range of 10–40 mM CTAB. We performed the time evolution spectra and transmission electron microscopy (TEM) characterizations. The results show a relatively competitive relationship between the CTAB/NaOL and HCl. Furthermore, a growth model has been proposed.

RESULTS AND DISCUSSION

Figure 1 shows the TEM and optical images of AuNR samples synthesized under different concentrations of NaOL. All the samples were synthesized at 10.0 mM CTAB, 0.14 mM $AgNO_3$, 0.30 ml HCl, and 0.04 ml seeds solution. To fully evaluate the influence of NaOL on the synthesis of AuNRs, we carried out a series of experiments and obtained the AuNR samples under 1.0–8.0 mM NaOL concentrations. It can be observed from Fig. 1 that when the NaOL concentration is very low (1–2 mM), large amounts of Au spheres were observed. As the NaOL concentration increased to 3–4 mM, high quality AuNRs were obtained. However, with the further increase of NaOL concentration (5–8 mM), Au spheres and other shapes of impurities like nanocubes increased.

Figure 2 shows the quality analysis of the AuNRs samples characterized in Fig. 1, including extinction spectra, parameters A_1/A_2, and Q. For A_1/A_2, Khlebstov *et al.*[25] used it to show the purity of AuNRs. A_1 is the absorbance of longitudinal LSPR peak, and A_2 is the absorbance of transverse LSPR/Au spheres peak. If there is a large quantity of Au sphere, the value of A_1/A_2 will be very low compared to the ideal AuNRs. We used Q, which is defined by $Q = \frac{\omega_0}{\Delta\omega} = \frac{\omega_0}{\omega_2-\omega_1} = \frac{\lambda_1\lambda_2}{\lambda_0(\lambda_2-\lambda_1)}$, where $\omega_0 = 2\pi c/\lambda_0$, $\omega_1 = 2\pi c/\lambda_1$, and $\omega_2 = 2\pi c/\lambda_2$. Here, c is the velocity of light in vacuum, λ_0 is the LSPR peak, and λ_1 and λ_2 are the wavelengths at half the maximum of the LSPR peak. The parameter strongly related to the bandwidth of the LSPR peaks was used to judge the monodispersity of the AuNRs samples.[24] Higher Q values have better size monodispersity. The normalized extinction spectra, A_1/A_2, and Q were shown in Fig. 2. The obtained AuNRs synthesized under 3 mM and 4 mM NaOL (10 mM CTAB) had both higher A_1/A_2 and Q values [Figs. 2(b) and 2(c)]. When we used 37 mM CTAB for AuNRs synthesis, the optimal concentration of NaOL needed to be increased to ~8 mM, or the high quality AuNRs could not be obtained (see Fig. S1). This kind of "bad-good-bad" phenomenon under the variation of 1–10 mM NaOL concentration was also found in other combinations of CTAB:NaOL (Fig. S2). The yield of AuNRs was calculated from the TEM images (Fig. 1), and the results were presented in Table I. They also followed this trend. All the above results have indicated that the ratio of CTAB:NaOL is important for an optimal growth condition for AuNRs. The reason for causing this "bad-good-bad" phenomenon will be discussed later.

To investigate the growth speed caused by different NaOL concentrations, we have recorded the growth process of the AuNRs samples by taking the extinction spectra at 30 min intervals. Figure S3 shows all the evolution of the AuNRs, with the concentration of NaOL from 1 to 8 mM. The extinctions at the longitudinal LSPR indicate the growth process. Figure 3 shows the intensity of LSPR vs growth time with NaOL concentrations of 1, 4, and 7 mM NaOL. When the NaOL concentration was low (1 mM), the growing speed of the AuNRs sample was so fast, and the extinction spectra became stable after only 60 min of growth. The transverse LSPR peak shown in the spectra [Fig. 2(a)] and the TEM image shown in Fig. 1(a) confirm the relatively high yield of Au sphere and bad monodispersity under 1 mM NaOL concentration. Compared with the growth speed of 4 mM NaOL and 7 mM NaOL, it was way too fast. Hence, the NaOL was likely to contribute to the symmetry breaking process.

In Fig. 3, the sample synthesized under 4 mM NaOL with the best quality among all the samples had moderate speed, which took 3 h for the sample to become stable. The growth speed between the 4 and 7 mM NaOL samples was close, which shows that the reduction of AA plays the leading role while the reduction effect of NaOL may have a limited contribution to the final growth process. However, the quality of the 4 mM NaOL sample was better than the 7 mM NaOL sample (higher Q and A_1/A_2). Hence, the NaOL should affect the AuNRs growth in another way. Ye *et al.* suggested that NaOL molecules might mediate the binding between CTAB surfactants and certain facets of growing NRs.[21] We compared the TEM results (shown in Fig. 1) of the AuNRs samples at 1, 4, and 7 mM NaOL, and the proportion of the rod-shaped Au nanocrystals was different. This may have confirmed the variation of growth speed affected by the NaOL concentration. The proportion of the rod shapes of AuNRs of the 4 and 7 mM NaOL samples was higher than 1 mM NaOL samples while the growth speed was lower. Similarly, although the overgrowth speed between the 4 and 7 mM NaOL samples was close, the proportion of the Au rods of 4 mM was higher than that of the

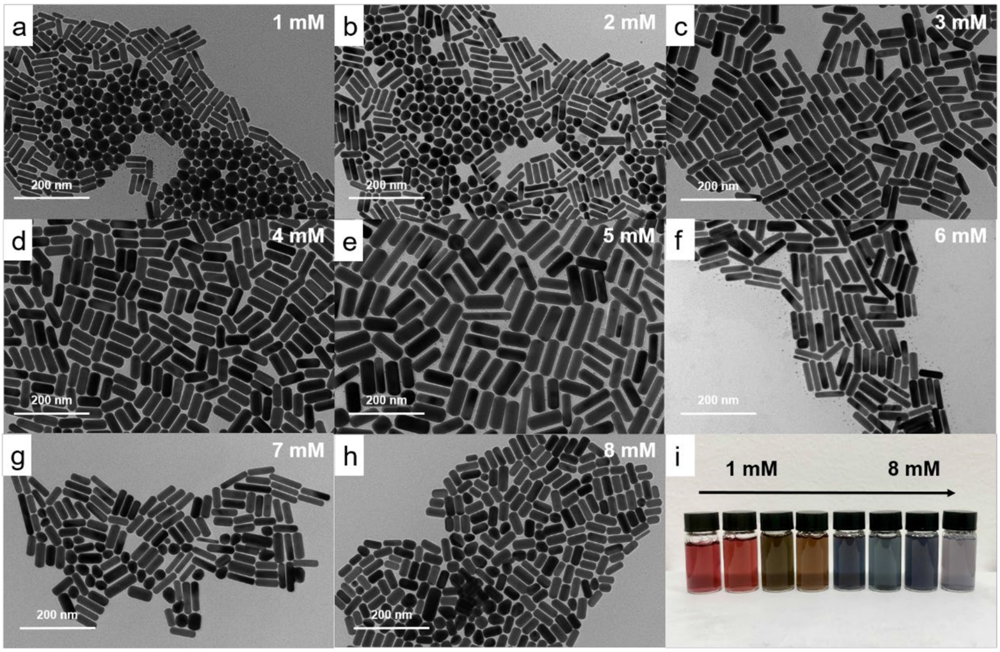

FIG. 1. TEM and optical images of AuNRs synthesized under different NaOL concentrations. The same parameters of the other reactants: CTAB (10.0 mM), $AgNO_3$ (0.14 mM), and HCl (0.30 ml) in the 25 ml final growth solution. (a)–(h) TEM images of AuNRs that synthesized in the NaOL concentrations of (a) 1.0 mM, (b) 2.0 mM, (c) 3.0 mM, (d) 4.0 mM, (e) 5.0 mM, (f) 6.0 mM, (g) 7.0 mM, and (h) 8.0 mM, respectively. The insets on the top right of (a)–(h) are the concentrations of NaOL. The average aspect ratios of AuNRs are (a) 3.5, (b) 3.6, (c) 3.2, (d) 2.8, (e) 3.2, (f) 4.1, (g) 3.3, and (h) 2.3, respectively. The average sizes (length and diameter) of AuNRs are (a) (51,15), (b) (56,15), (c) (68,22), (d) (68,25), (e) (75,24), (f) (76,19), (g) (67,21), and (h) (51,23). All size parameters mentioned above were given by measuring at least 100 of AuNRs. (i) Optical image of the obtained samples shown in (a)–(h). The NaOL concentration increases from 1.0 to 8.0 mM (from left to right).

7 mM NaOL samples. We think CTAB and NaOL contributed differently. CTAB packed densely on the {110} facet of AuNRs, guiding the growth direction. A suitable addition of NaOL greatly increased the yield of the rod-shaped Au nanocrystals (see Fig. 1). It worked like a buffer to slow down the growth rate of Au seeds; hence, it is most likely to affect certain facets at the early stage of Au seeds. Therefore, CTAB may contribute to both early seeds and the overgrowth process while NaOL mainly contributes to the former. It formed the best combination and enhancement at moderate molar ratios of CTAB:NaOL.

To get a better understanding of the cooperative interaction between CTAB and NaOL, we have carried out further synthesis experiments under different combinations of CTAB:NaOL. The spectra of all the samples were shown in Fig. S2. In order to compare the qualities of the obtained AuNRs at different LSPR peaks, the A_1/A_2 of all the AuNRs samples were calculated, as shown in

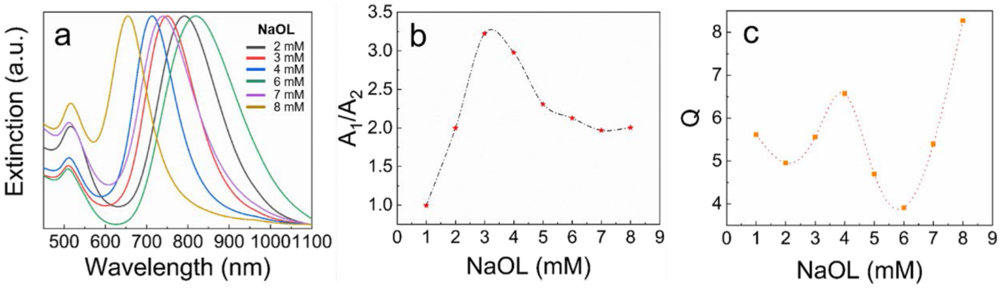

FIG. 2. Quality analysis of the AuNRs samples shown in Fig. 1(a). Normalized extinction spectra of AuNRs synthesized under different NaOL concentrations including: 2.0 mM NaOL, black curve, 747 nm; 3.0 mM NaOL, red curve, 791 nm; 4.0 mM NaOL, blue curve, 751 nm; 6.0 mM NaOL, green curve, 819 nm; 7.0 mM NaOL, purple curve, 740 nm; and 8.0 mM NaOL, golden curve, 655 nm. The spectra of the samples synthesized under 1.0 and 5.0 mM NaOL were deleted because of overlapping. (b) The A_1/A_2 of the AuNRs. (c) The parameter Q of the AuNRs samples.

TABLE I. Aspect ratio, length, diameter, yield, A_1/A_2, Q, and LSPR of AuNRs samples shown in Figs. 1 and 2.

CTAB (mM)	NaOL (mM)	A_1/A_2	Q	LSPR (nm)	Aspect ratio	Length (nm)	Diameter (nm)	Yield from TEM (%)	Figure number
10.0	1.0	1.0	5.6	747	3.5 ± 0.6	51.1 ± 6.1	15.0 ± 2.1	41	1(a)
10.0	2.0	2.0	5.0	791	3.6 ± 0.6	56.1 ± 7.3	15.7 ± 2.2	52	1(b)
10.0	3.0	3.2	5.6	750	3.2 ± 0.5	67.9 ± 8.1	21.5 ± 2.8	>99	1(c)
10.0	4.0	3.0	6.6	714	2.8 ± 0.4	68.3 ± 6.4	24.8 ± 2.1	>99	1(d)
10.0	5.0	2.3	4.7	750	3.2 ± 0.8	75.2 ± 12.3	24.1 ± 4.7	92	1(e)
10.0	6.0	2.1	4.0	819	4.1 ± 1.0	76.0 ± 12.4	19.1 ± 3.5	97	1(f)
10.0	7.0	2.0	5.4	740	3.3 ± 0.8	66.8 ± 10.8	20.9 ± 3.3	76	1(g)
10.0	8.0	2.0	8.3	655	2.3 ± 0.4	51.5 ± 8.0	23.3 ± 3.2	81	1(h)

Fig. S4. The solid marks represented the A_1/A_2 of the AuNRs samples were higher than 3 while the hollow ones represented lower. Similarly, the Q of the AuNRs samples was shown in Fig. S5. Solid marks mean that the parameter Q was higher than 5, while hollow ones mean lower. We overlapped all the solid marks of Figs. S4 and S5 and the results were shown in Fig. 4. The full details of the synthesis conditions were listed in Table S1. "-" in Table S1 means the LSPR peaks either higher than 1100 nm or non-exist. According to Fig. 1, the best samples with 3 and 4 mM NaOL concentrations were set at 5 for Q and 3 for A_1/A_2. If higher values were set, no good samples will be chosen. However, if lower values were set, too many samples will be selected, and it is hard to distinguish the excellent samples. Therefore, a proper value of Q and A_1/A_2 was selected. From 10 to 40 mM CTAB and 1 to 10 mM NaOL, the tuning of high quality AuNRs growth over this large concentration range was not as smooth as expected, until we started to change the amount of HCl. When the addition of HCl was fixed, for example, 0.3 ml, it worked at the concentration combinations of 10 mM CTAB and 3–5 mM NaOL. However, if we increased the concentration of the binary surfactants, the qualities of the obtained samples decreased distinctly.

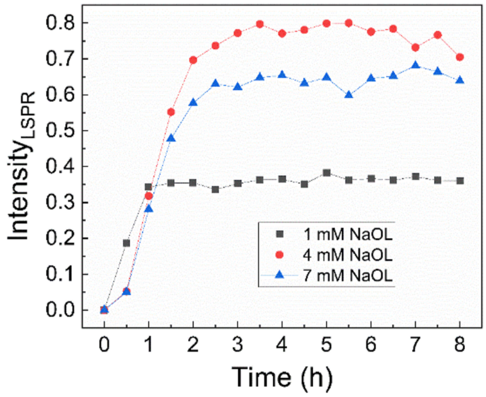

FIG. 3. The intensity of LSPR vs the growth time, with NaOL concentration of 1.0 mM (black squares), 4.0 mM (red dots), and 7.0 mM (blue triangles), while keeping other parameters the same. The extinction spectra were recorded from 0.5 to 8 h at 30 min intervals.

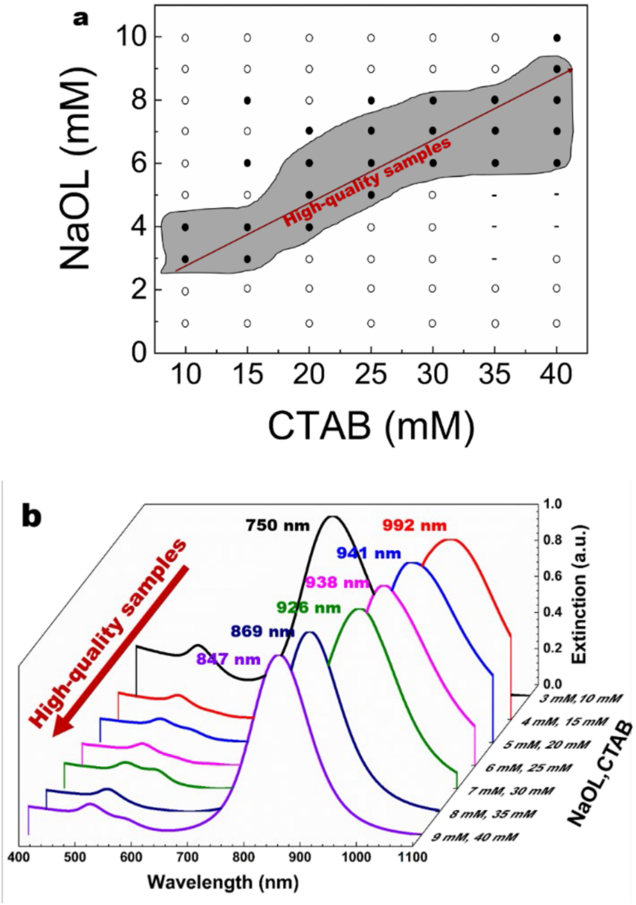

FIG. 4. (a) Scatterplot showing the quality variation of the obtained AuNRs caused by the concentration combinations of two surfactants. X axis is the concentration of CTAB, and y axis is the concentration of NaOL. The quality was measured by both parameters A_1/A_2 and Q, and solid marks represented both the parameters Q of the obtained AuNRs were higher than 5 and the A_1/A_2 were higher than 3 while the hollow ones represented lower. " - " means the LSPR peaks longer than 1100 nm. (b) Normalized extinction spectra of the high-quality samples marked by the red arrow in Fig. 4(a). The LSPR peaks were given with the corresponding color.

Under this circumstance, high quality AuNRs samples were only obtained under the corresponding decrease of HCl. Following this procedure, the attempts to adjust various addition of HCl under different CTAB:NaOL were made, and finally, the suitable parameters were determined. A domain with samples of good quality was finally demarcated. In this domain, a continuous increase through the red arrow was marked. It indicated that when we adjust the amount of HCl properly, the relationship between CTAB:NaOL for good quality AuNRs samples can be near-linear. Thus, the NaOL concentration needs to be increased when the CTAB concentration was high, exhibiting a match of the surfactant's concentration. Moreover, at a fixed CTAB concentration, it is possible to obtain high quality AuNRs in a certain range of NaOL concentrations. Figure 4(b) shows the normalized extinction spectra of the high-quality samples marked by the red arrow of Fig. 4(a). It should be noted that these samples were the best in their series and are marked in red in Table S1. There is a distinct blue-shift of LSPR peaks except for the sample synthesized under 10 mM CTAB and 3 mM NaOL. This exception may due to the high addition of HCl, which greatly weakened the reducibility of AA.

To fully explain these phenomena mentioned above, we proposed a growth model discussing the Au from seeds to different shapes of nanocrystals under low, moderate, and high NaOL concentrations circumstances, as shown in Scheme 1. The seed-mediated synthesis of the AuNRs could be understood as a dynamic reduction/diffusion process with the influence between different energy and growing states of Au nanocrystals in the growth solution. First, we discuss the diversity of Au seeds in our growth model, which strongly influenced the final products. Park *et al.*[26] measured the size of the 90 min aged Au seeds, which were presented in a bimodal distribution, from <1.0 to >5.5 nm. Walsh *et al.*[27] demonstrated that the seeds were found to exist in three kinds of crystalline structures including single crystal, twinned, and multiply twinned. Hence, at the very beginning of the reaction, these two characteristics showed the diversity between each seed, resulting in different "starting points." The second key point was the diffusion of Au^+ in the growth solution. This was primarily determined by the Au^+ gradient. According to Fick's first law, the diffusion rate (J) can be described by the $J = -D\nabla c$, where D is the diffusion coefficient and ∇c is the concentration gradient of Au^+. Moreover, D is given by the Stokes–Einstein equation $D = k_b T/6\pi\eta$, where k_b is the Boltzmann constant, T is the temperature, and η is the viscosity of the solvent.

It was illustrated in Scheme 1 that in the initial state (after the final addition of seed solution and stirring), the reactants, especially seeds and Au^+, should be homogeneously dispersed in the growth solution. Based on the assumption that the NaOL mediated the binding between CTAB and certain facets. The binding strength is proportional to the concentration of NaOL.[21] This state evolved into three different growth scenarios according to different NaOL concentrations. Therefore, at low NaOL concentration, symmetry breaking may occur soon in the fast-growing seeds. This closely fitted in the "pop-corn" theory;[28] after breaking through an energy barrier, they grew very fast. It brought the high consumption of Au^+ around these fast-growing seeds and creates a high concentration gradient. According to Fick's first law, this caused a strong diffusion of Au^+ from the nearby area of other seeds with low/moderate growing speed to this fast-growing seed. In this situation, it seemed

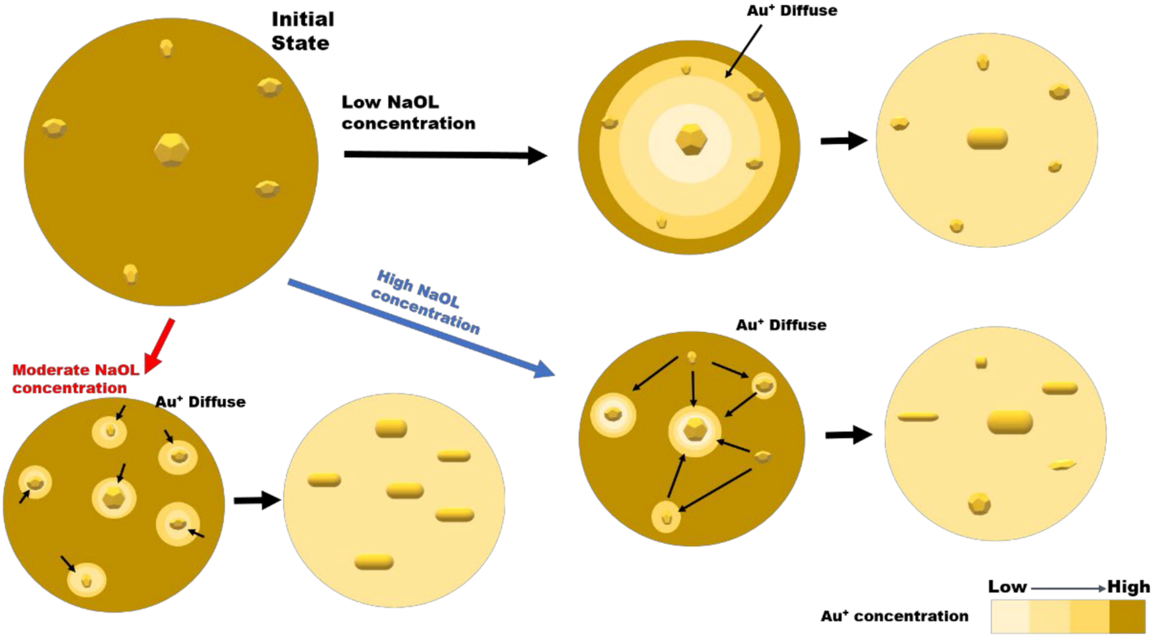

SCHEME 1. The growth model of AuNRs from seeds to different shapes of nanocrystals under low, moderate, and high concentrations of NaOL. The other synthesis conditions were fixed.

like the Au^+ around other seeds were occupied by the fast-growing seeds, created the Au^+ imbalance, and finally led to the shape duality of "rod" and "sphere."

For moderate NaOL concentration, the reduction rate was moderate and optimal. The Au^+ concentration gradients around most of the seeds were lower than the former situation. Hence, the diffusion was mild, seeds interfered less with each other, and most of them grew independently. Finally, the AuNRs with the best monodispersity was obtained. When the NaOL concentration was high, the reduction rate was relatively slow, and some Au seeds may not be able to get over the energy barrier of the symmetry breaking process while some Au seeds did. Some Au seeds needed more time to complete the symmetry breaking process. The concentration distribution of Au^+ was more chaotic, and the mutual influence between seeds was large, resulting in a large polydispersity in the final size and morphology of the obtained samples. They may also explain why we needed to decrease the amount of HCl when the concentration of the binary surfactants increased. When the pH gets lower, a part of the ascorbic acid is transformed into its fully protonated, nonreactive form, which cannot be oxidized under the used synthesis conditions.[29] Therefore, the reducibility of ascorbic acid increases with an increase in pH, to keep a balance of reduction and diffusion. Gallagher *et al.* used Fick's first law to explain the anisotropic growth of single AuNRs.[30] In this work, we considered the whole system and its interactions.

The self-assembly behavior of the surfactants above critical micelles concentration also affected the diffusion rate by changing the viscosity η of the solution. Hence, when the surfactant concentration was high, it formed more micelles, thus slowing down the diffusion rate.[31]

It showed the key factor of the appearance of "monodispersity" and shape impurities. In a word, the varying Au^+ concentration gradients that are affected by the differential growth progress of every single seed ultimately cause significant shape and size diversity of the obtained Au nanocrystals. This model may give another angle to design better experimental parameters and a deeper understanding of the seed-mediated synthesis method.

CONCLUSION

We have demonstrated the influence of NaOL in the seed-mediated synthesis of AuNRs using binary surfactants CTAB and NaOL. At a fixed synthetic parameter, the results indicate that the concentration of NaOL should be moderate; otherwise, the qualities of the obtained AuNRs samples will decrease. The evolution of the extinction spectra with time and the TEM images confirmed that the low NaOL concentrations led to the formation of many Au spheres and affected the symmetry breaking process, while the synthesis process under high concentrations of NaOL may be more chaotic, resulting in AuNRs with low size monodispersity. Therefore, the growth speed of AuNRs should be moderate. Moreover, we discovered the ideal ranges of the NaOL concentrations under different CTAB concentrations (10–40 mM), and these results indicated that the NaOL concentration should increase when the CTAB concentration increases. The addition of HCl should be changed to satisfy a good growth condition. We introduced a growth model based on the balance of diffusion and reduction in order to explain the experimental results. The existence of "monodispersity" of AuNRs may come from the mutual interference between seeds through the synthesis process. In a word, the imbalance of the reduction rate vs the diffusion rate of Au^+ will magnify the diversity of initial seeds, which finally leads to the polydispersity of Au rods and other Au nanocrystals. This work has given a deeper understanding of the relationship and interference of the binary surfactant in the synthesis process. These results have the potential to guide future experiments on nanomaterials synthesis.

EXPERIMENTAL SECTION

Materials

All chemicals were obtained from commercial suppliers and used without further purification. Hexadecyltrimethylammonium bromide (CTAB, >99.0%), chloroauric acid ($HAuCl_4$), and L-ascorbic acid (>99.99% metals basis) were purchased from Macklin. Silver nitrate ($AgNO_3$, >99.8%), sodium oleate (NaOL, >99.88%), and sodium borohydride ($NaBH_4$, 98%) were purchased from Aladdin.

Synthesis of gold nanorods

Preparation of seeds solution: 0.25 ml of 10.0 mM $HAuCl_4$ was added to 10.0 ml 0.1M CTAB solution. Then, the 0.6 ml of 10.0 mM $NaBH_4$ (freshly prepared with cold water) was added under vigorous stirring. The color of the solution changed from yellow to brownish yellow. The seed solution was aged at 30 °C for 30 min before use.

The growth solution was prepared by adding 2.5 ml of 0.1M CTAB in a 40 ml scintillation vial. Then, 0.014 g of NaOL was dissolved in 21.25 ml of warm water (45–50 °C) in the same scintillation vial. When the solution cooled down to 30 °C, 0.9 ml of 4.0 mM $AgNO_3$ solution was added. The mixture was kept undisturbed at 30 °C for 15 min after which 10.0 mM of 0.25 ml $HAuCl_4$ was added. The solution became colorless after 90 min of stirring. To adjust the pH, 0.3 ml of HCl (37 wt. % in water) was added. 75 μl of 64 mM ascorbic acid and 0.04 ml of seed solution were added after 15 min. Finally, the resultant solution was left undisturbed at 30 °C overnight for nanorod growth. The detailed experimental parameters are listed in Tables I and S1.

Characterization

Optical extinction spectra were recorded with a UV-1900i spectrophotometer (SHIMADZU, Japan) with a 10 mm optical path. Transmission electron microscopy (TEM) images were obtained with an HT-7700 microscope (HITACHI, JAPAN) operating at 100 kV. The particle sizes of the AuNRs were measured from TEM images, whereby >100 particles were measured for each sample.

Preparation of TEM samples: 1.5 ml of AuNRs solution was centrifuged at 6000 rpm for 10 min. Then, the supernatant was removed, and a certain amount of water was added (always keep the concentration of CTAB higher than its CMC, ~1 mM) and ultrasonicated for 10 min (power 400 W). The processes were repeated three times. Finally, 5 μl of the solution in the centrifuge tube was dropped onto a carbon-coated 300 square-mesh copper grid and allowed to dry slowly in the air.

SUPPLEMENTARY MATERIAL

See the supplementary material for more extinction spectra (both common and time-evolution), tables with all the synthesis parameters, and scatter plots.

ACKNOWLEDGMENTS

The authors acknowledge financial support from the National Natural Science Foundation of China (NSFC, Grant Nos. 61905056, 91938201, and 61871169), the National Key R & D Program of China (Grant No. 2018YFE0207500), the Zhejiang Provincial Natural Science Foundation of China (Grant Nos. LY19E020011 and LZ20F010004), and the Project of Ministry of Science and Technology (Grant No. D20011).

AUTHOR DECLARATIONS

Conflict of Interest

The authors have no conflicts to disclose.

Author Contributions

Ming-Zhang Wei: Conceptualization (equal); Data curation (equal); Formal analysis (equal); Investigation (equal); Methodology (equal); Writing – original draft (equal); Writing – review & editing (equal). **Tian–Song Deng**: Conceptualization (equal); Data curation (equal); Formal analysis (equal); Funding acquisition (equal); Investigation (equal); Methodology (equal); Supervision (equal); Validation (equal); Visualization (equal); Writing – review & editing (equal). **Qi Zhang**: Formal analysis (equal); Investigation (equal). **Xi Chen**: Investigation (equal). **Zhiqun Cheng**: Funding acquisition (equal). **Shiqi Li**: Funding acquisition (equal). **Yi-Jie Gu**: Investigation (equal); Visualization (equal).

DATA AVAILABILITY

The data that support the findings of this study are available within the article and its supplementary material.

REFERENCES

[1] L. Tian, M. K. Su, F. F. Yu, Y. Xu, X. Y. Li, L. Li, H. L. Liu, and W. H. Tan, Nat. Commun. **9**, 12 (2018).

[2] E. A. Kwizera, R. O'Connor, V. Vinduska, M. Williams, E. R. Butch, S. E. Snyder, X. Chen, and X. Huang, Theranostics **8**, 2722–2738 (2018).

[3] G. Fu, D.-W. Sun, H. Pu, and Q. Wei, Talanta **195**, 841–849 (2019).

[4] C. L. Zhang, K. P. Lv, H. P. Cong, and S. H. Yu, Small **16**, 1904785 (2020).

[5] M. Kim, J. H. Lee, and J. M. Nam, Adv. Sci. **6**, 1900471 (2019).

[6] N. Elahi, M. Kamali, and M. H. Baghersad, Talanta **184**, 537–556 (2018).

[7] T. T. Hoang Thi, V. D. Cao, T. N. Q. Nguyen, D. T. Hoang, V. C. Ngo, and D. H. Nguyen, Mater. Sci. Eng. C **99**, 631–656 (2019).

[8] T. He, C. Jiang, J. He, Y. Zhang, G. He, J. Wu, J. Lin, X. Zhou, and P. Huang, Adv. Mater. **33**, 2008540 (2021).

[9] Y.-S. Chen, Y. Zhao, S. J. Yoon, S. S. Gambhir, and S. Emelianov, Nat. Nanotechnol. **14**, 465–472 (2019).

[10] T. Kim, Q. Zhang, J. Li, L. Zhang, and J. V. Jokerst, ACS Nano **12**, 5615–5625 (2018).

[11] Y. Liu, P. Bhattarai, Z. Dai, and X. Chen, Chem. Soc. Rev. **48**, 2053–2108 (2019).

[12] W. Ni, X. Kou, Z. Yang, and J. Wang, ACS Nano **2**, 677–686 (2008).

[13] B. Nikoobakht and M. A. El-Sayed, Chem. Mater. **15**, 1957–1962 (2003).

[14] N. R. Jana, L. Gearheart, and C. J. Murphy, Adv. Mater. **13**, 1389–1393 (2001).

[15] H. Chen, L. Shao, Q. Li, and J. Wang, Chem. Soc. Rev. **42**, 2679–2724 (2013).

[16] A. Gole and C. J. Murphy, Chem. Mater. **16**, 3633–3640 (2004).

[17] S. R. Jackson, J. R. McBride, S. J. Rosenthal, and D. W. Wright, J. Am. Chem. Soc. **136**, 5261–5263 (2014).

[18] D. K. Smith, N. R. Miller, and B. A. Korgel, Langmuir **25**, 9518–9524 (2009).

[19] D. K. Smith and B. A. Korgel, Langmuir **24**, 644–649 (2008).

[20] X. Ye, Y. Gao, J. Chen, D. C. Reifsnyder, C. Zheng, and C. B. Murray, Nano Lett. **13**, 2163–2171 (2013).

[21] X. Ye, C. Zheng, J. Chen, Y. Gao, and C. B. Murray, Nano Lett. **13**, 765–771 (2013).

[22] Y. Xu, L. Chen, X. Ye, X. Wang, J. Yu, Y. Zhao, M. Cao, Z. Xia, B. Sun, and Q. Zhang, Nano Res. **10**, 2146–2155 (2017).

[23] G. González-Rubio, V. Kumar, P. Llombart, P. Díaz-Núñez, E. Bladt, T. Altantzis, S. Bals, O. Peña-Rodríguez, E. G. Noya, and L. G. Macdowell, ACS Nano **13**, 4424–4435 (2019).

[24] M.-Z. Wei, T.-S. Deng, Q. Zhang, Z. Cheng, and S. Li, ACS Omega **6**, 9188–9195 (2021).

[25] B. N. Khlebtsov, V. A. Khanadeev, J. Ye, G. B. Sukhorukov, and N. G. Khlebtsov, Langmuir **30**, 1696–1703 (2014).

[26] K. Park, L. F. Drummy, R. C. Wadams, H. Koerner, D. Nepal, L. Fabris, and R. A. Vaia, Chem. Mater. **25**, 555–563 (2013).

[27] M. J. Walsh, S. J. Barrow, W. Tong, A. M. Funston, and J. Etheridge, ACS Nano **9**, 715–724 (2015).

[28] J. A. Edgar, A. M. Mcdonagh, and M. B. Cortie, ACS Nano **6**, 1116–1125 (2012).

[29] B. D. Busbee, S. O. Obare, and C. J. Murphy, Adv. Mater. **15**, 414–416 (2003).

[30] R. Gallagher, X. Zhang, A. Altomare, D. Lawrence, N. Shawver, N. Tran, M. Beazley, and G. Chen, Nano Res. **14**, 1167–1174 (2021).

[31] X. Ye, L. Jin, H. Caglayan, J. Chen, G. Xing, C. Zheng, V. Doan-Nguyen, Y. Kang, N. Engheta, C. R. Kagan, and C. B. Murray, ACS Nano **6**, 2804–2817 (2012).

Supplementary Material for:

New rule and growth model for the synthesis method of gold nanorods with binary surfactant CTAB&NaOL

Ming-Zhang Wei[1], **Tian–Song Deng**[1,*], **Qi Zhang**[1], **Xi Chen**[1], **Zhiqun Cheng**[1], **Shiqi Li**[1], **Yi-Jie Gu**[1]

[1]College of Electronics and Information Engineering, Hangzhou Dianzi University, No. 1158, 2nd Avenue, Baiyang Street, Hangzhou 310018, China

[*]Email: dengts@pku.edu.cn

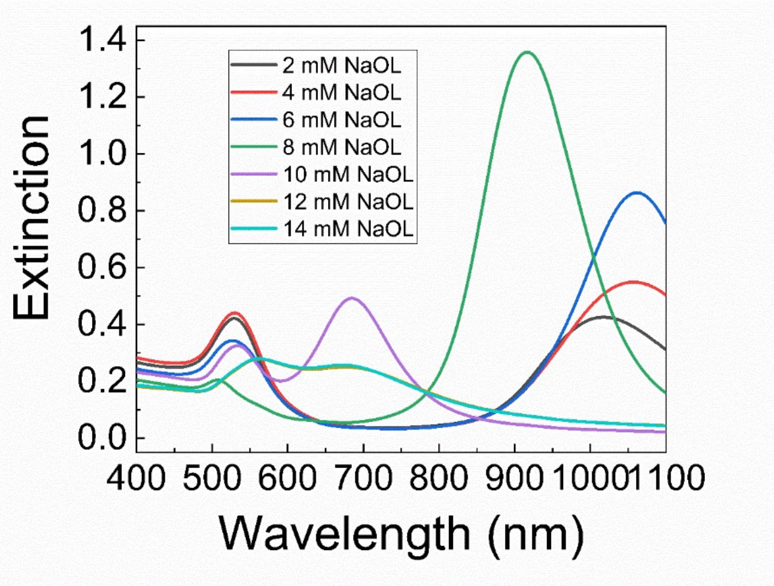

Figure S1. Extinction spectra of AuNRs synthesized under 37 mM CTAB and 2-14 mM of NaOL. The amounts of other reactants are 0.14 mM $AgNO_3$, 0.11 mL of HCl and 0.04 mL of seed solution. The volume of the final growth solution is 25 mL.

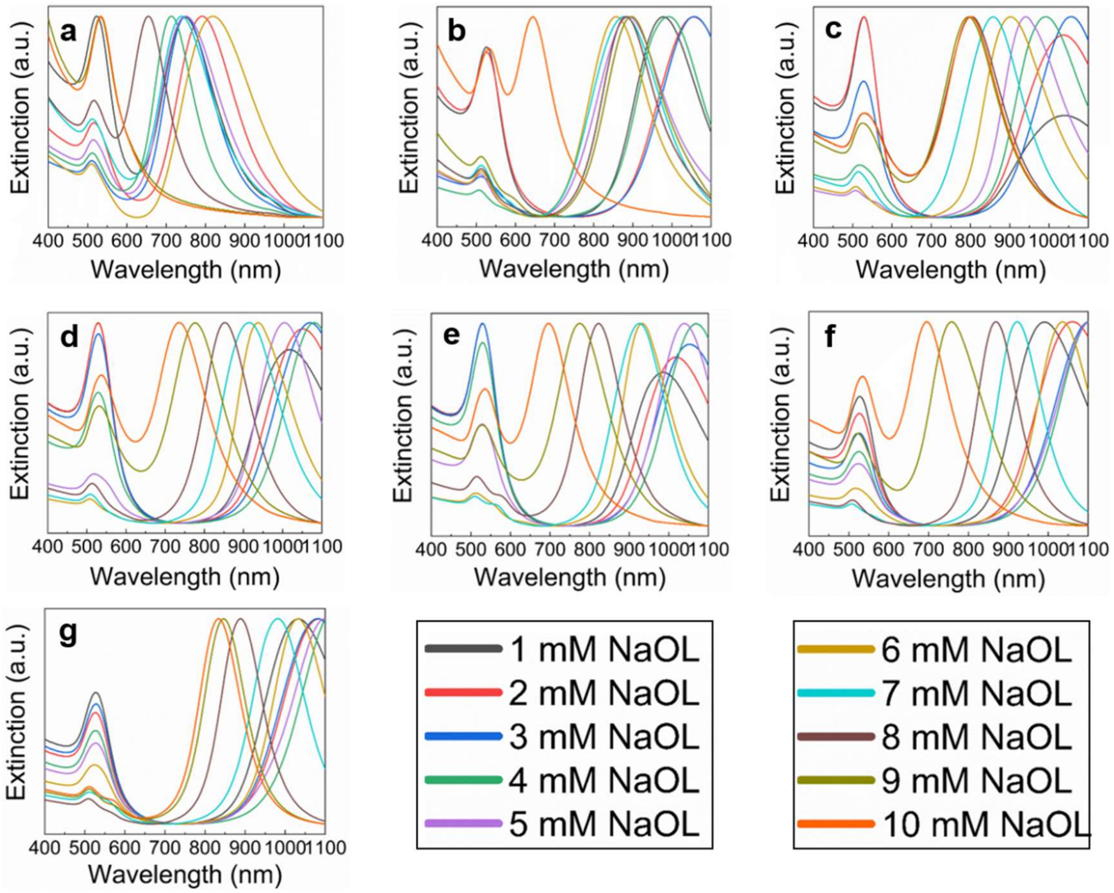

Figure S2. The normalized extinction spectra of AuNRs synthesized under different concentration of CTAB (a) 10.0 mM; (b) 15.0 mM; (c) 20.0 mM; (d) 25.0 mM; (e) 30.0 mM; (f) 35.0 mM; (g) 40.0 mM. At each CTAB concentration, the concentration of NaOL varied from 1.0 mM to 10.0 mM. The other experimental parameters can be found in Table S1.

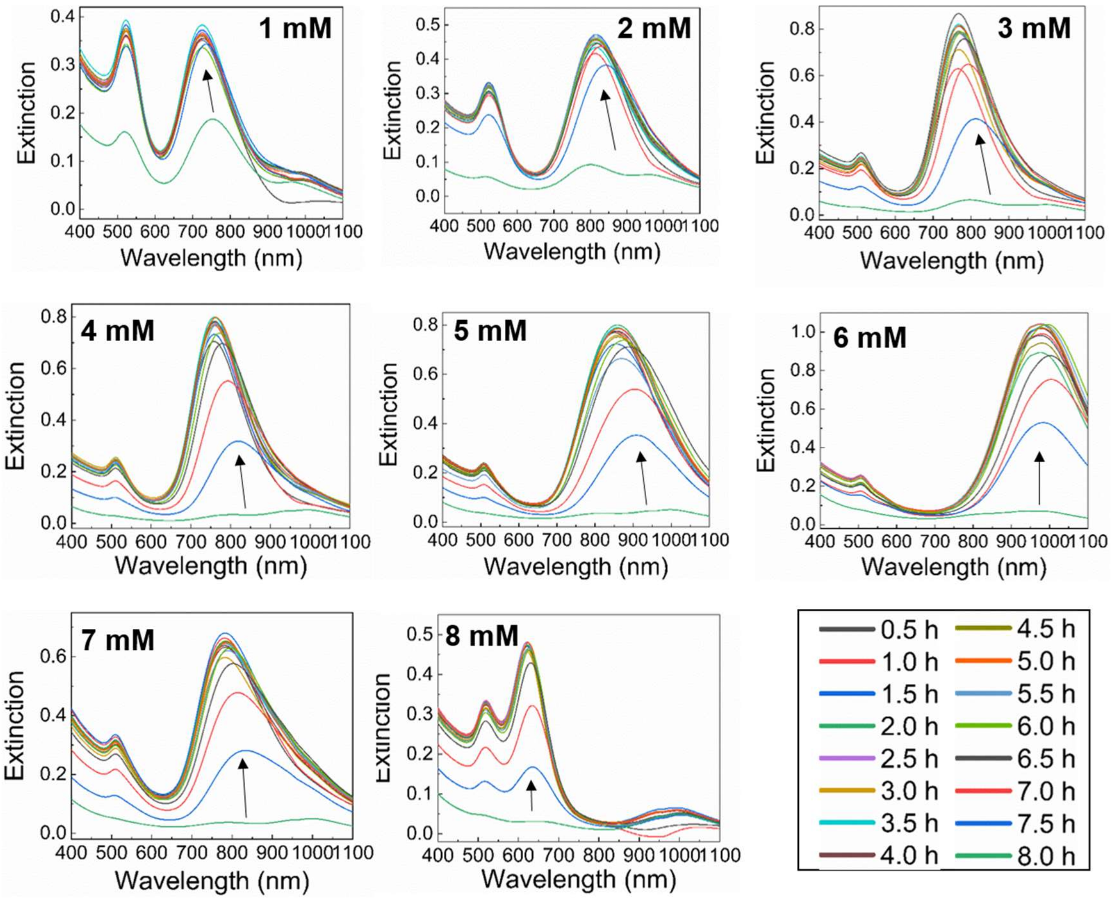

Figure S3. The evolution of the AuNRs samples shown in Figure 1, characterized at 30 min intervals with a time period of 8 h. The NaOL concentration was varied from 1.0 mM to 8.0 mM. The other experimental parameters can be found in Table S1.

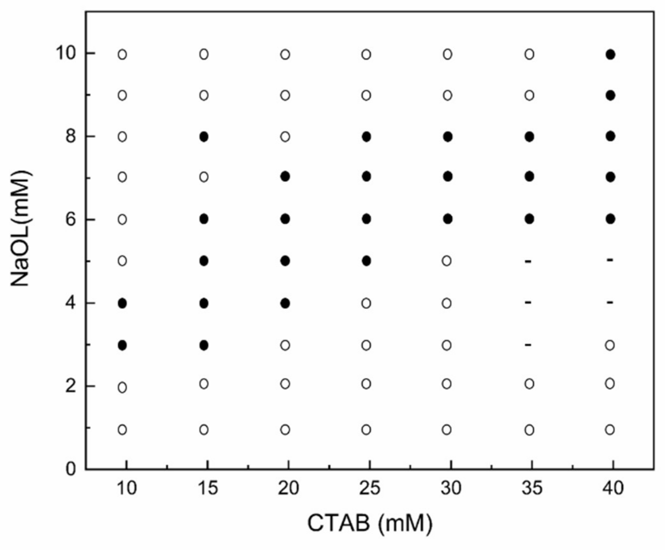

Figure S4. Scatterplot showing the quality variation of the obtained AuNRs based on A_1/A_2. X-axis is the concentration of CTAB, Y-axis is the concentration of NaOL. The solid marks represented the A_1/A_2 of the AuNRs samples were higher than 3 while the hollow ones represented lower.

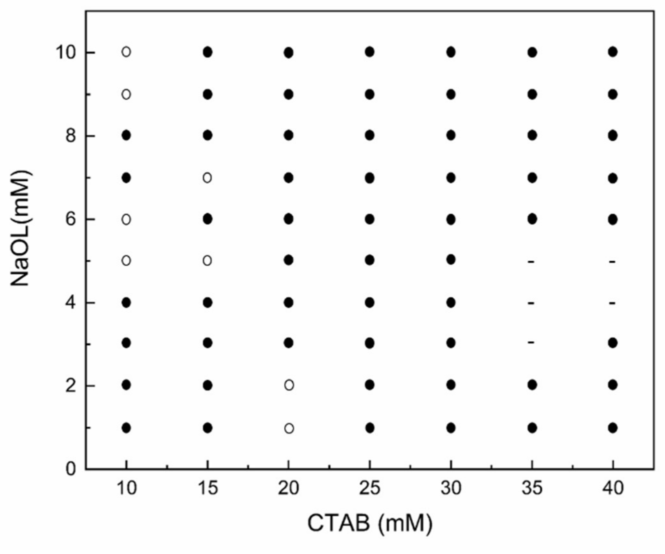

Figure S5. Scatterplot showing the quality variation of the obtained AuNRs based on *Q* values. X-axis is the concentration of CTAB, Y-axis is the concentration of NaOL. The solid marks represented the *Q* of the AuNRs samples were higher than 5 while the hollow ones represented lower.

Table S1. Detailed parameters of AuNRs synthesized at different amount of CTAB, NaOL, HCl, $AgNO_3$, and seed solution. (The volume of the final growth solution is 25 mL). High-quality samples were bold and italic, as shown below.

CTAB (mM)	NaOL (mM)	HCl (mL)	$AgNO_3$ (mM)	Seed (mL)	LSPR Peak (nm)	Figure Number
10.0	1.0	0.3	0.14	0.04	748	Fig. 1a
10.0	2.0	0.3	0.14	0.04	791	Fig. 1b
10.0	***3.0***	***0.3***	***0.14***	***0.04***	***751***	***Fig. 1c***
10.0	4.0	0.3	0.14	0.04	714	Fig. 1d
10.0	5.0	0.3	0.14	0.04	750	Fig. 1e
10.0	6.0	0.3	0.14	0.04	819	Fig. 1f
10.0	7.0	0.3	0.14	0.04	740	Fig. 1g
10.0	8.0	0.3	0.14	0.04	655	Fig. 1h
10.0	9.0	0.3	0.14	0.04	-	Fig. S2a
10.0	10.0	0.3	0.14	0.04	-	Fig. S2a
15.0	1.0	0.2	0.14	0.04	978	Fig. S2b
15.0	2.0	0.2	0.14	0.04	1055	Fig. S2b
15.0	3.0	0.2	0.14	0.04	1057	Fig. S2b
15.0	***4.0***	***0.2***	***0.14***	***0.04***	***992***	***Fig. S2b***
15.0	5.0	0.2	0.14	0.04	890	Fig. S2b
15.0	6.0	0.2	0.14	0.04	859	Fig. S2b
15.0	7.0	0.2	0.14	0.04	877	Fig. S2b
15.0	8.0	0.2	0.14	0.04	883	Fig. S2b
15.0	9.0	0.2	0.14	0.04	897	Fig. S2b
15.0	10.0	0.2	0.14	0.04	644	Fig. S2b
20.0	1.0	0.14	0.14	0.04	1041	Fig. S2c
20.0	2.0	0.14	0.14	0.04	1037	Fig. S2c
20.0	3.0	0.14	0.14	0.04	1056	Fig. S2c

20.0	4.0	0.14	0.14	0.04	993	Fig. S2c
20.0	***5.0***	***0.14***	***0.14***	***0.04***	***941***	***Fig. S2c***
20.0	6.0	0.14	0.14	0.04	902	Fig. S2c
20.0	7.0	0.14	0.14	0.04	857	Fig. S2c
20.0	8.0	0.14	0.14	0.04	804	Fig. S2c
20.0	9.0	0.14	0.14	0.04	795	Fig. S2c
20.0	10.0	0.14	0.14	0.04	801	Fig. S2c
25.0	1.0	0.13	0.14	0.04	1018	Fig. S2d
25.0	2.0	0.13	0.14	0.04	1053	Fig. S2d
25.0	3.0	0.13	0.14	0.04	1070	Fig. S2d
25.0	4.0	0.13	0.14	0.04	1081	Fig. S2d
25.0	5.0	0.13	0.14	0.04	1005	Fig. S2d
25.0	***6.0***	***0.13***	***0.14***	***0.04***	***938***	***Fig. S2d***
25.0	7.0	0.13	0.14	0.04	914	Fig. S2d
25.0	8.0	0.13	0.14	0.04	853	Fig. S2d
25.0	9.0	0.13	0.14	0.04	777	Fig. S2d
25.0	10.0	0.13	0.14	0.04	736	Fig. S2d
30.0	1.0	0.10	0.14	0.04	987	Fig. S2e
30.0	2.0	0.10	0.14	0.04	1017	Fig. S2e
30.0	3.0	0.10	0.14	0.04	1051	Fig. S2e
30.0	4.0	0.10	0.14	0.04	1069	Fig. S2e
30.0	5.0	0.10	0.14	0.04	1040	Fig. S2e
30.0	6.0	0.10	0.14	0.04	934	Fig. S2e
30.0	***7.0***	***0.10***	***0.14***	***0.04***	***926***	***Fig. S2e***
30.0	8.0	0.10	0.14	0.04	823	Fig. S2e
30.0	9.0	0.10	0.14	0.04	775	Fig. S2e
30.0	10.0	0.10	0.14	0.04	696	Fig. S2e

35.0	1.0	0.08	0.14	0.04	991	Fig. S2f
35.0	2.0	0.08	0.14	0.04	1062	Fig. S2f
35.0	3.0	0.08	0.14	0.04	-	Fig. S2f
35.0	4.0	0.08	0.14	0.04	-	Fig. S2f
35.0	5.0	0.08	0.14	0.04	-	Fig. S2f
35.0	6.0	0.08	0.14	0.04	1036	Fig. S2f
35.0	7.0	0.08	0.14	0.04	923	Fig. S2f
35.0	***8.0***	***0.08***	***0.14***	***0.04***	***869***	***Fig. S2f***
35.0	9.0	0.08	0.14	0.04	758	Fig. S2f
35.0	10.0	0.08	0.14	0.04	695	Fig. S2f
40.0	1.0	0.08	0.14	0.04	1033	Fig. S2g
40.0	2.0	0.08	0.14	0.04	1083	Fig. S2g
40.0	3.0	0.08	0.14	0.04	1087	Fig. S2g
40.0	4.0	0.08	0.14	0.04	-	Fig. S2g
40.0	5.0	0.08	0.14	0.04	-	Fig. S2g
40.0	6.0	0.08	0.14	0.04	1032	Fig. S2g
40.0	7.0	0.08	0.14	0.04	982	Fig. S2g
40.0	8.0	0.08	0.14	0.04	889	Fig. S2g
40.0	***9.0***	***0.08***	***0.14***	***0.04***	***847***	***Fig. S2g***
40.0	10.0	0.08	0.14	0.04	835	Fig. S2g